

Correlation Method of Dangerous Objects Detection for Aviation Security Systems

Maksym Zaliskyi¹, Serhii Migel¹, Alina Osipchuk¹, and Denys Bakhtiiarov¹

¹National Aviation University, 1 Lubomyr Huzar ave., Kyiv, 03058, Ukraine

Abstract

Aviation security services have significant value for aviation safety. Aviation security services include personnel and technical equipment for dangerous and prohibited object detection. The X-ray screening system is the main equipment for baggage contain determining. The X-ray security devices give the possibility to detect weapons, including handguns, knives, and others. The high value of the probability of false detection of X-ray screening systems requires the development of new methods of image processing. Therefore, this paper concentrates on the synthesis and analysis of methods for handgun recognition while operating the X-ray screening system. The synthesis is based on a special image processing technique using a comparison of verified images with etalon images. During this, we use the correlation coefficient to determine verified object similarity with etalons inside the database and define their mutual rotation and resizing. The analysis is associated with computer modeling for estimating probabilistic characteristics of method efficiency.

Keywords

Image processing, recognition, correlation coefficient, baggage screening, aviation security

1. Introduction

One of the main problems in civil aviation is to increase the safety and regularity of aircraft flights [1]. Different reasons can affect safety. The general approach considers two types of threats that include unintentional and deliberate behaviors [2]. The unintentional behavior does not involve acts of unlawful interference. This case refers to random events occurring in the aviation system [3]. Such events can be connected with all supported resources for flight processes [4]. There are various factors associated with unintentional behavior, but the most important of them are:

1. Reliability of aviation equipment and the possibility of random and gradual failures, damages, and malfunctions occurrence [5, 6].
2. Human factors, including maintenance personnel and aircraft pilots [7].
3. Organizational factors and environmental conditions [8, 9].

The deliberate behavior of terrorists and criminals can significantly reduce the level of aviation safety. To counter such events, the aviation security service operates at airports. Each passenger and their baggage must be checked before they enter the aircraft.

The aviation security service includes personnel and technical equipment to implement the function of dangerous and prohibited object detection. Personnel must be appropriately trained. Technical equipment creates a system of levels, on each of which different threats must be detected and eliminated [10]. For these purposes, personnel uses screening equipment, detectors of explosives, video surveillance devices, access control systems, alarm systems, and others.

A new challenge in the era of digital information technology development and utilization is protection against cyberterrorism. This threat can be realized using different types of cyberattacks, spreading false information aimed to impair airport operations [11–13].

CPITS 2023: Workshop on Cybersecurity Providing in Information and Telecommunication Systems, February 28, 2023, Kyiv, Ukraine
EMAIL: maximus2812@ukr.net (M. Zaliskyi); migel_S@i.ua (S. Migel); alina.osipchuk2012@gmail.com (A. Osipchuk); bakhtiiaroff@tks.nau.edu.ua (D. Bakhtiiarov)
ORCID: 0000-0002-1535-4384 (M. Zaliskyi); 0000-0001-5807-2013 (S. Migel); 0000-0002-9053-2072 (A. Osipchuk); 0000-0003-3298-4641 (D. Bakhtiiarov)



© 2023 Copyright for this paper by its authors. Use permitted under Creative Commons License Attribution 4.0 International (CC BY 4.0).

CEUR Workshop Proceedings (CEUR-WS.org)

2. Literature Review and Problem Statement

Following international requirements and recommendations, screening inspection measures should be organized at the airports. Screening usually contains three or five levels. To analyze the internal structure of the baggage, the personnel of the aviation security service uses X-ray devices [14]. The experience of equipment operation shows that the main disadvantage of modern X-ray systems is a high level of probability of false alarms [15, 16]. In some cases, this probability can reach levels of 0.3, which means that three of ten items of baggage need an additional inspection. It is clear that this negatively affects the speed of security control and reduces the level of throughput of airport passenger traffic.

To improve the efficiency of X-ray screening systems, designers use two approaches. The first approach is related to the modernization of equipment operation processes [17, 18]. Such modernization can be applied to all elements of the operation system, including maintenance and repair processes, parameter monitoring and control of the technical condition of equipment, and others [19]. The second approach involves the usage of more efficient data processing procedures [20, 21]. The data in the aviation security X-ray system are images of scanned items of baggage. Therefore, the data are a two-dimensional array of discrete values corresponding to the shades of the intensity of image pixels.

The literature considers many different methods of image processing for X-ray systems. The research [22] concentrates on classical methods of image processing. The methods of processing can be divided into the detection methods for the given object, methods of noise filtration, methods for the definition of object contours, methods of highlighting the image in a given area of the color gamut, and others [23, 24].

Effective data processing methods can significantly simplify security control processes based on automating the detection of dangerous objects [25].

Research [15] concentrates on the algorithm for the recognition of dangerous objects based on an implicit shape model. The authors developed the visual vocabulary of objects for detection. The proposed approach has good probabilistic characteristics of detection for shuriken and razor blades (probability of correct detection is

0.97 ... 0.99 and probability of false alarm is 0.02 ... 0.06) and sufficient probabilistic characteristics for handguns (corresponding probabilities are equal to 0.89 and 0.18, respectively). Paper [26] presents a similar approach to weapon recognition. In addition, the authors proposed a component-based strategy with fast robust properties. Research [27] deals with the weapon detection algorithm while screening vehicles. The proposed approach consists of the following steps: pre-processing, database usage, obtained image binarization, detection of edges, and weapon detection after edges comparison with information from the database. Conducting an experiment study gave authors the possibility to conclude about 80% accuracy of the developed methodology.

A new trend in image processing is the usage of artificial intelligence techniques and Neural Networks (NNs). In the branch of X-ray image processing, the most convenient type of NN is Convolutional NN (CNN). A literature search gives many examples of CNN utilization for the tasks of dangerous object detection.

Publication [28] deals with the research of the pre-trained CNN using the paradigm of transfer learning. Such CNN is used for the recognition of handguns and provides high efficiency in terms of the probability of false alarms. The authors obtained the value of corresponding probability approximately equal to 0.0021.

Paper [29] presents an efficiency analysis of CNN utilization for the recognition of different objects. The possible ways of CNN modernization for X-ray systems are considered in the publication [30]. We can conclude that CNN is an effective and robust method for the recognition of weapons and other prohibited objects, but it has weakness in the necessity of high enough computing time and power [31].

The literature considers different approaches for data processing and detection in many fields of study, for example, those given in publications [32–37], which could be adapted for automated X-ray screening systems. Data processing techniques in the field of detection can be applied for tasks of object recognition on X-ray images.

Mentioned analysis of the literature shows insufficient probabilistic characteristics of detection while X-ray security system image processing. Therefore, the aim of this paper is a synthesis of a new method for dangerous object recognition, an analysis of the efficiency of the proposed method, and the formation of recommendations for this method's improvement.

3. Methodology

The X-ray security system consists of a transmitter and receiver of X-ray radiation. The transmitter unit contains a radiation source (X-ray tube), a power supply unit, and collimators (to form the scan beam). The receiver unit contains a detector line, optical-to-electrical and electrical-to-optical signal converters, a unit for image processing, and a device for information display. Baggage is placed on a conveyor and moved through the scanning area between the transmitter and receiver.

The detector line of the receiver records one of the parameters of attenuated radiation that propagates through the baggage. Received parameter values are encoded in gamut luminosity or grayscale. In this situation, the received parameter is a three-dimensional function of the coordinates (x, y, z) . However, since the monitor of the X-ray security system displays a two-dimensional image, we will consider the brightness function to be two-dimensional for a further solution to our problem. Let the brightness function is $\Psi(x, y)$. In this case, the abscissa and ordinate will indicate a specific image pixel on the monitor of the X-ray security system.

The problem of improving the unit for image processing is not new. However, this problem is still relevant today due to several reasons:

1. A constant increase in the variety of prohibited and dangerous items.
2. The possibility of noises that distort the quality of the image.
3. An increase in the complexity of airport structure and the increasing level of airport passenger traffic.
4. Limitation for time to make correct decisions on aviation security measures.

There are two ways to the improvement of the unit for image processing associated with the hardware and software. However, both approaches require new efficient methods of data processing. In these conditions, statistical and filtering techniques are very relevant.

To examine the proposed method, this research uses computer modeling and statistical simulation. In addition, it should be noted that our approach is at the first stage of development, so some limitations will be used.

The flowchart of data processing procedures while recognizing dangerous objects on the X-ray security system image is shown in Fig. 1.

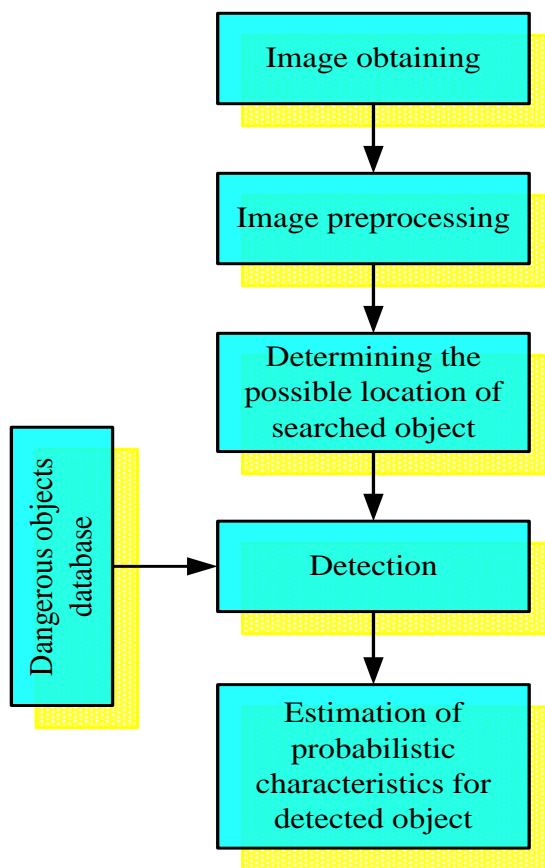


Figure 1: The flowchart of data processing procedures

The first procedure is image obtaining. This procedure is implemented in an X-ray security system based on encoding the level of attenuated radiation into the brightness. The image has the form of a two-dimensional array with the corresponding value of brightness. The metal objects completely absorb radiation, and then the value in the array for this case will be equal to zero. The maximum possible value in the array corresponds to receiving radiation without attenuation.

The second procedure is signal preprocessing. This procedure concentrates on the initial preparation of the image for subsequent operations. Preprocessing can contain image noise filtration, image dimensions change, selection of the objects with given attenuation of radiation, and others. For example, if we want to recognize handguns, we will select only metal objects with complete attenuation of the signal. However, such selection decreases the quality of dangerous object detection, because weapons can be produced using 3D printers and other materials.

The next procedure is possible to position determination for the searched object. This procedure can be implemented using different

transformations to decision space, various clustering techniques, spatial spectra calculation, and others.

The detection procedure assumes decisive statistics calculation and comparison of their values with a threshold. The threshold can be computed using some priori information, for example about the probability of false alarm for given statistical characteristics of noise.

To synthesize the efficient algorithm for different object detection, the reference database of searched object masks can be used. In the general case, the masks give the possibility to train the detector and improve the quality of detection. The X-ray security system must contain filter banks for different dangerous objects. This study uses seven types of etalons for handguns that need to be detected. The etalons description is shown in Fig. 2.



Figure 2: Etalons for detection

The last procedure of data processing is an estimation of probabilistic characteristics for detected objects. This procedure assumes calculation receiver operating characteristics for different noise situations, calculation of error matrix, and others.

In this paper, we concentrate on only techniques for handgun detection. This technique is based on the correlation coefficient calculation of analyzed images and etalons.

Before explaining the step-by-step procedure of detection, let's introduce limitations:

1. The object of the search is the handgun.
2. The preprocessing procedure filter all noises in the image.
3. The object of search has an arbitrary angle of rotation and arbitrary scale factor.
4. The area of possible location of a handgun is selected in the image.
5. The handgun can be produced using 3D printers.

The calculations of all steps for the detection procedure were carried out in the MathCAD program.

Consider the step-by-step procedure of detection.

Step 1. Reading images of selected areas of analyzed items and etalons. It is possible to perform simultaneous studies for all etalons. For simplicity, this methodology presents only one of them. The example of the selected area and etalon 6 images are shown in Fig. 3.

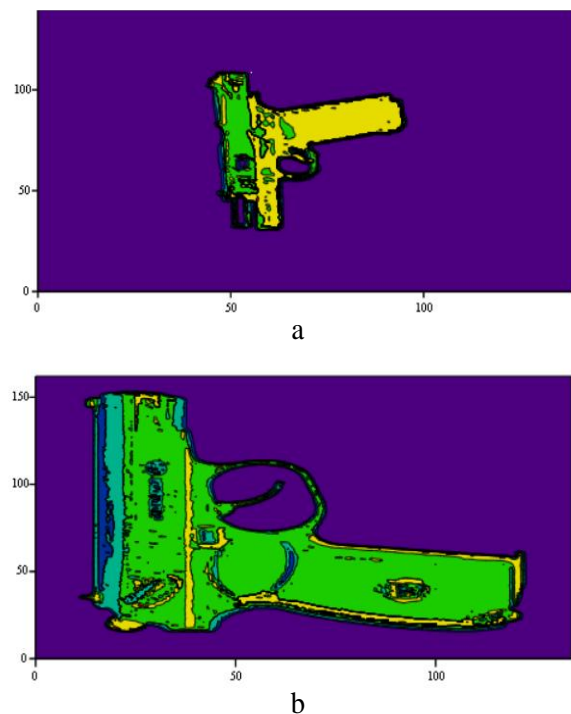


Figure 3: Images in MathCAD: a) possible area of handgun location; b) image of etalon 6

In the MathCAD program, images were obtained using the built-in operator *read_image()*. In addition, at this step, it is possible to distort the image by adding noise to it. Two noise generators

have been implemented: Gaussian and Rayleigh. Noise parameters can be adjusted, and it is possible to estimate the signal-to-noise ratio.

Step 2. Image binarization. To speed up the computing process, it may be useful to filter out pixels of small amplitudes—insignificant ones. The remaining pixels can be considered as significant. To implement this procedure, the thresholds for etalons and analyzed images were chosen. The results of the calculation are matrices $B(x, y)$ that contain zeroes and ones.

The example of binarization for images presented in Fig. 3 is shown in Fig. 4.

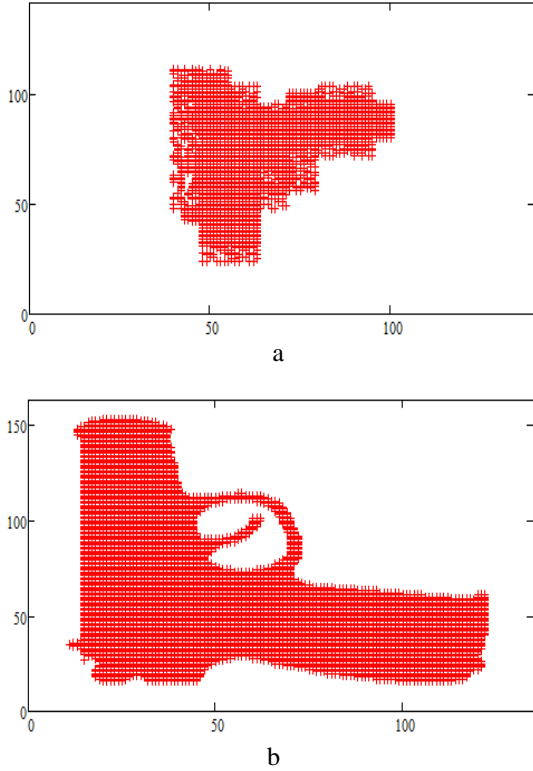


Figure 4: Images after binarization: a) tested image; b) image of etalon 6

Step 3. Moving the center of the etalons to the center of the analyzed image. For this purpose, first of all, it is necessary to estimate the centers of images obtained in Step 2. To apply statistical data processing methods to our image, we will introduce the following analogy. Let the image is formed by a set of points (columns in three-dimensional space), and the pixel intensity (brightness function $\Psi(x, y)$) indicates the number of points in each of the pixels. If the total quantity of points is N_p , then the center coordinates will be

$$x_c = \frac{1}{N_p} \sum_{x=1}^{N_x} \sum_{y=1}^{N_y} x \Psi(x, y) B(x, y),$$

$$y_c = \frac{1}{N_p} \sum_{x=1}^{N_x} \sum_{y=1}^{N_y} y \Psi(x, y) B(x, y),$$

where N_x and N_y are image dimensions.

Obtained estimate of the center is weighed center with taking into account pixel intensity.

The results of the calculation generate centers for analyzed images ($x_c; y_c$) and etalons ($x_{cEi}; y_{cEi}$).

The image movement is realized using the matrix method of graphics processing [38]. The translation matrix in this case will be

$$T_{Ei} = \begin{pmatrix} 1 & 0 & x_c - x_{cEi} \\ 0 & 1 & y_c - y_{cEi} \\ 0 & 0 & 1 \end{pmatrix}.$$

The coordinates of each pixel of the etalon are transformed according to the equation

$$\begin{pmatrix} x_{Em} \\ y_{Em} \\ 1 \end{pmatrix} = \begin{pmatrix} 1 & 0 & x_c - x_{Ei} \\ 0 & 1 & y_c - y_{Ei} \\ 0 & 0 & 1 \end{pmatrix} \begin{pmatrix} x_E \\ y_E \\ 1 \end{pmatrix}.$$

Step 4. Estimation of Rotation Angle (RA).

This step consists of two parts.

Step 4. Part 1. Determining radial matrix.

It is assumed that the distance between the center of the image and the arbitrary point of the image in the radial matrix will not be displayed on a linear scale, but using the power function. In this case, the number of distance rings between any two arbitrary points of the same image with different scale factors will be the same, which will allow comparing them by correlation coefficient using a sliding window.

The dimensions of the radial matrix correspond to the quantity of distance rings N_d and the quantity of discrete scan sectors N_s . Also, it is necessary to choose the parameter d of the power function.

The radial proportion factor K_{rp} is equal to the difference in the area of the sector covering the given distance ring and the sector covering all previous rings except the given one. For i^{th} distance ring, the radial proportion factor can be presented as follows

$$K_{rpi} = \frac{\pi}{N_s} \left(2^{\frac{2i+1}{d}} - 2^{\frac{2i-1}{d}} \right).$$

The radial matrix gives the possibility to represent the polar coordinates in a rectangular shape and to simplify the calculation of the correlation coefficient. The example of radial matrices for analyzed image and etalon 6 from Fig. 3 in the case of 108 rings of distance, 512 discrete sectors, and $d = 16$ is shown in Fig. 5.

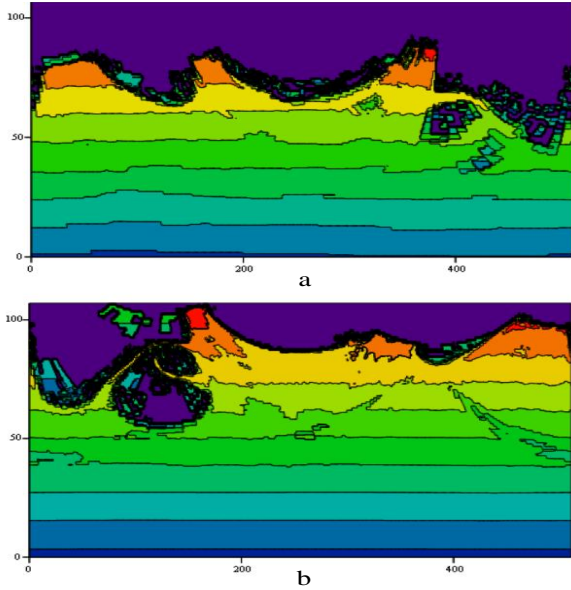


Figure 5: Radial matrices for images: a) tested image; b) image of etalon 6

Step 4. Part 2. Solving optimization task for the correlation coefficient. To make it possible to calculate the correlation coefficient, we computed the sums of all distances in the radial matrices for all possible sectors. The example of obtained dependencies is shown in Fig. 6.

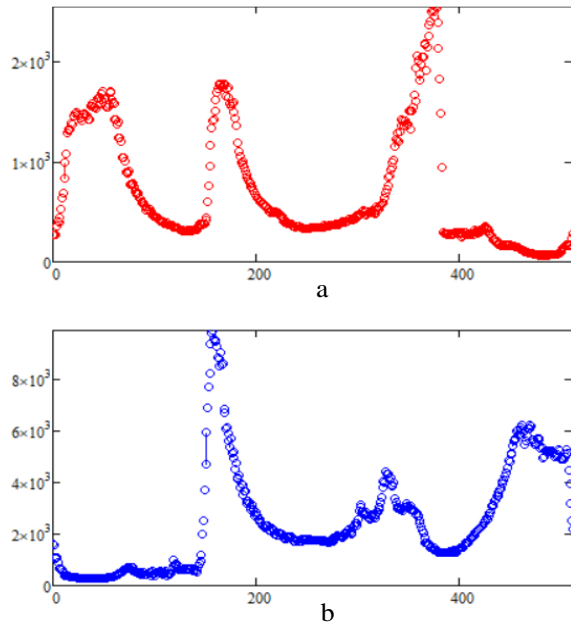


Figure 6: Sums of distances for radial matrices of images: a) tested image; b) image of etalon 6

The movement of the etalon image to the position of the analyzed one may require not only rotation but also reflection. Therefore, we created a reversible matrix of accumulated sums of distances in the discrete sectors for the etalon image to further use it in sliding processing for step-by-step evaluation of the correlation with a

reflected copy and to make a decision about the need to perform reflection transformation.

The next stage of calculation is an estimation of the correlation coefficient. For this purpose, direct and reverse matrices were extended to two complete rotations. After that, we used the estimation of the correlation coefficient in sliding windows that moved along extended matrices.

Fig. 7 presents the dependence of the correlation coefficient estimates on the rotation angle for direct and reverse sliding. Visual analysis of dependencies shows the existence of a global maximum for both cases. These values are equal to 0.7 and 0.821 for direct and reverse sliding, respectively.

The comparison of global maximums of the correlation coefficient allows making decisions about image reflection. In this numerical case, reverse sliding provides the greater value of the global maximum, so the etalon image should be reflected.

To perform reflection transformation, we used the matrix equation with reflection matrix about the x -axis of the following type

$$M = \begin{pmatrix} 1 & 0 & 0 \\ 0 & -1 & 0 \\ 0 & 0 & 1 \end{pmatrix}.$$

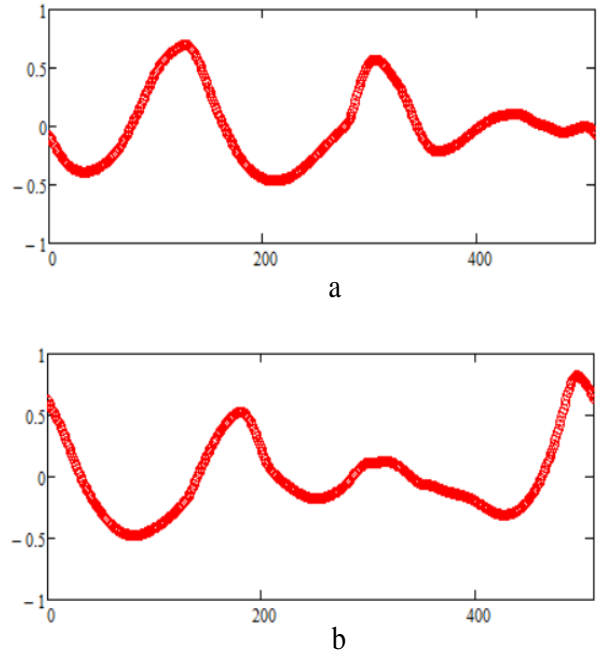


Figure 7: Estimates of the correlation coefficient for (a) direct sliding and (b) reverse sliding

Then we can estimate the RA α . This angle corresponds to the argument of a maximum of global maximums for the correlation coefficient for direct and reverse sliding, i.e.

$$\alpha = -\frac{2\pi}{N_s} \arg \max(r_{\text{dir}}(j), r_{\text{rev}}(j)),$$

where j is several discrete scan sectors, $r_{\text{dir}}(j)$ and $r_{\text{rev}}(j)$ are correlation coefficients for direct and reverse sliding, respectively.

For considered numerical example, the estimate of RA is equal to -6.075 radians.

To perform rotation of etalons, we used the matrix equation with rotation matrix about the center of the coordinate system of the following type

$$R_{Ei} = \begin{pmatrix} \cos \alpha & -\sin \alpha & 0 \\ \sin \alpha & \cos \alpha & 0 \\ 0 & 0 & 1 \end{pmatrix}.$$

It should be noted that to implement this procedure, etalon images were moved to the coordinate system origin, reflected in case of necessity, rotated, and moved back to the initial point. Therefore, this operation requires two translation matrices of the following types

$$T_1 = \begin{pmatrix} 1 & 0 & -x_c \\ 0 & 1 & -y_c \\ 0 & 0 & 1 \end{pmatrix}, \quad T_2 = \begin{pmatrix} 1 & 0 & x_c \\ 0 & 1 & y_c \\ 0 & 0 & 1 \end{pmatrix}.$$

The complete transformation matrix for Step 4 will take the following form

$$T_\alpha = \begin{cases} T_2 M R_{Ei} T_1, & \text{if } \max(r_{\text{dir}}) < \max(r_{\text{rev}}), \\ T_2 R_{Ei} T_1, & \text{otherwise.} \end{cases}$$

After performing the matrix calculation, we can obtain the following result

$$\begin{aligned} & \text{a) if } \max(r_{\text{dir}}) < \max(r_{\text{rev}}), \\ & \quad T_2 M R_{Ei} T_1 = \\ & = \begin{pmatrix} \cos \alpha & -\sin \alpha & x_c - x_c \cos \alpha + y_c \sin \alpha \\ -\sin \alpha & -\cos \alpha & y_c + x_c \sin \alpha + y_c \cos \alpha \\ 0 & 0 & 1 \end{pmatrix}; \\ & \text{b) if } \max(r_{\text{dir}}) \geq \max(r_{\text{rev}}), \\ & \quad T_1 R_{Ei} T_2 = \\ & = \begin{pmatrix} \cos \alpha & -\sin \alpha & x_c - x_c \cos \alpha + y_c \sin \alpha \\ \sin \alpha & \cos \alpha & y_c - x_c \sin \alpha - y_c \cos \alpha \\ 0 & 0 & 1 \end{pmatrix}. \end{aligned}$$

The example of the transformation result is shown in Fig. 8. Visual analysis of obtained radial matrices shows the approximately same shape of both dependencies.

Step 5. Estimation of the scale factor. This step is associated with solving the optimization task for the correlation coefficient.

For this purpose, we perform direct and reverse linear movement of images of radial transformations of the etalon image relative to the tested one and vice versa with sliding correlation coefficient estimation.

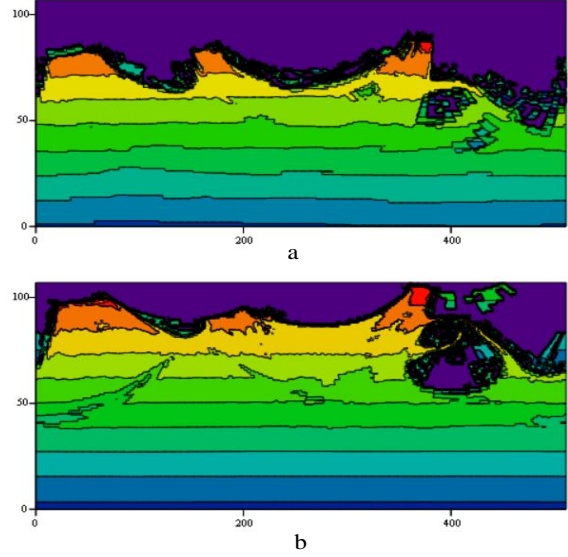


Figure 8: Radial matrices for images: a) tested image; b) image of etalon 6

In this case, we use the property of radial matrices, which is connected with the fact that the number of distance rings between any two arbitrary points of the same image with different scaling factors is the same, which allows estimating the correlation coefficient using a sliding distance window. The success of the described procedure requires sliding the radial matrix of larger objects relative to the radial matrix of smaller objects. However, since the size of each of the objects is unknown, it is necessary to check both sliding options.

Fig. 9 presents the dependence of the correlation coefficient estimates on the scale factor for both sliding options. Visual analysis of dependencies shows the existence of maximum in one of two cases. The maximum values are equal to 0.69 and 0.108 for direct and reverse sliding, respectively.

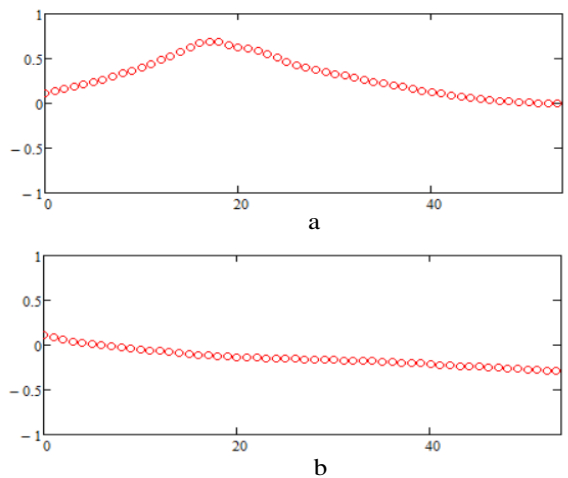


Figure 9: Estimates of the correlation coefficient for (a) direct sliding and (b) reverse sliding

The comparison of maximums of the correlation coefficient allows estimating the scale factor s . This factor corresponds to the argument of the maximum correlation coefficient for direct and reverse sliding, i.e.

$$s = 2^{\frac{\arg \max(r_{\text{dir}}(j), r_{\text{rev}}(j))}{d}}$$

For considering numerical examples the estimate of the scale factor is equal to—0.479.

To perform the scaling procedure, we used the matrix equation with a scaling matrix of the following type

$$S_{Ei} = \begin{pmatrix} s & 0 & 0 \\ 0 & s & 0 \\ 0 & 0 & 1 \end{pmatrix}.$$

It should be noted that to implement this procedure, etalon images were moved to the coordinate system origin, scaled, and moved back to the initial point. The complete transformation matrix for Step 5 will take the following form

$$T_s = T_1 S_{Ei} T_2 = \begin{pmatrix} s & 0 & x_c - sx_c \\ 0 & s & y_c - sy_c \\ 0 & 0 & 1 \end{pmatrix}.$$

An example of the transformation result is shown in Fig. 10.

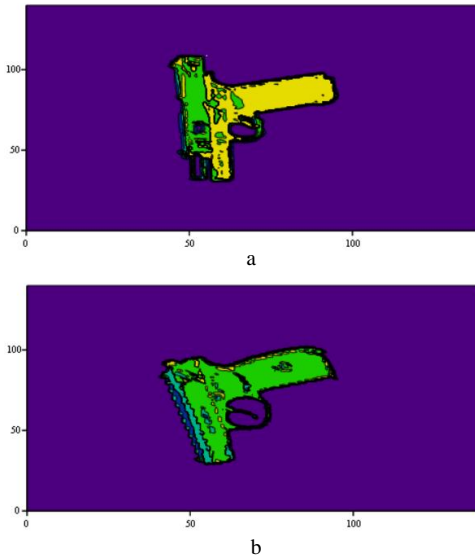


Figure 10: Images after all transformations: a) tested image; b) image of etalon 6

Step 6. Final decision-making. This procedure consists of two operations. The first operation is a calculation of the correlation coefficient between the analyzed image and the transformed image of the etalon. The second operation is a comparison of the correlation coefficient with the threshold. If the calculated correlation is greater than the threshold, the decision on dangerous object presence will be made.

The main problem is the threshold value determination. In this research, the threshold value was calculated based on computer modeling. The value of the threshold corresponds required value of the probability of a false alarm. For our study, we computed the approximate value of the threshold for a decision about handgun presence for a 0.01 probability of a false alarm. This threshold is approximately equal to 0.71. In future research, we will try to find the value of the threshold taking into account noise influence based on statistical simulation.

For the presented numerical example, the final correlation coefficient is equal to 0.799. This value exceeds the threshold, so we have the correct detection of handguns.

The flowchart of the proposed method for handgun detection is shown in Fig. 11.

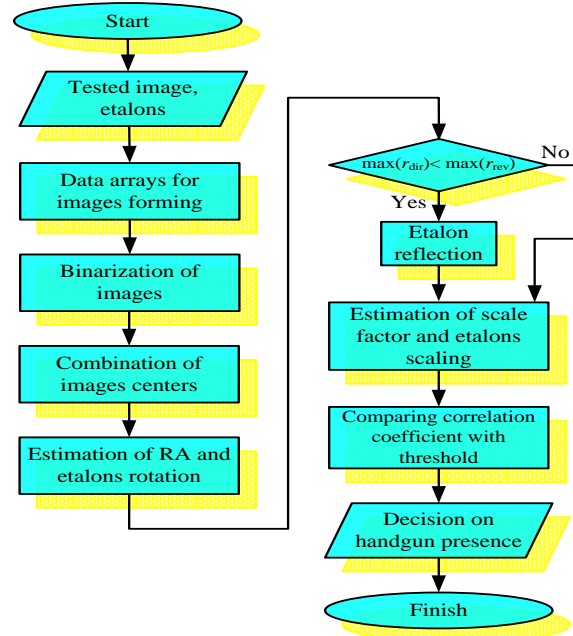


Figure 11: The flowchart of a proposed procedure for the detection

4. Results and Discussion

To estimate the efficiency of the proposed method of detection, it is necessary to perform an analysis. In classical interpretation, the analysis of the detector assumes the calculation of receiver operating characteristics. However, according to the introduced limitations we process the image without noise. In this case, the analysis concentrates on the calculation of a matrix of correct and erroneous decisions while handgun recognition.

The analysis was carried out using the designed program in MathCAD. To test the possible decision-making, two types of tested images were generated. The first type is one of the etalon images with an arbitrary angle of rotation and arbitrary scale factor. The second type is one of the tested images, including other dangerous objects (weapons) and non-dangerous objects. The basic types of tested images are shown in Fig. 12.

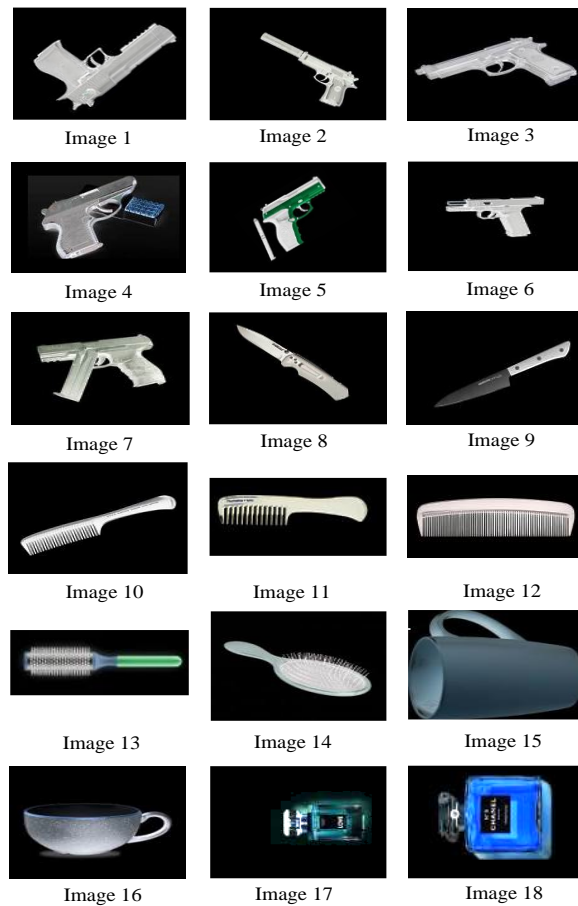


Figure 12: The images for detector testing

The results of correlation coefficient calculation in the case of etalon (E) and tested image (I) recognition are given in Table 1 and Table 2, respectively.

Table 1
Correlation coefficient for etalons

r	E1	E2	E3	E4	E5	E6	E7
E1	1	0.78	0.59	0.53	0.87	0.79	0.91
E2	0.78	1	0.63	0.51	0.74	0.76	0.79
E3	0.59	0.64	1	0.44	0.59	0.55	0.59
E4	0.5	0.58	0.49	1	0.55	0.66	0.57
E5	0.85	0.72	0.56	0.53	1	0.75	0.88
E6	0.76	0.75	0.53	0.56	0.74	1	0.77
E7	0.89	0.77	0.56	0.53	0.87	0.77	1

Table 2
The correlation coefficient for tested images

r	E1	E2	E3	E4	E5	E6	E7
I1	0.86	0.75	0.62	0.53	0.87	0.75	0.91
I2	0.7	0.61	0.56	0.53	0.69	0.6	0.72
I3	0.88	0.78	0.59	0.5	0.83	0.74	0.88
I4	0.68	0.66	0.59	0.4	0.63	0.62	0.68
I5	0.67	0.68	0.6	0.51	0.61	0.66	0.64
I6	0.76	0.78	0.71	0.63	0.73	0.8	0.76
I7	0.51	0.59	0.48	0.55	0.54	0.56	0.54
I8	0.5	0.46	0.45	0.36	0.46	0.42	0.51
I9	0.52	0.46	0.48	0.35	0.48	0.45	0.52
I10	0.5	0.42	0.4	0.28	0.45	0.44	0.48
I11	0.47	0.4	0.41	0.2	0.45	0.41	0.47
I12	0.43	0.39	0.4	0.26	0.41	0.42	0.42
I13	0.42	0.38	0.22	0.22	0.37	0.35	0.4
I14	0.7	0.58	0.66	0.61	0.65	0.65	0.69
I15	0.49	0.47	0.41	0.36	0.44	0.5	0.5
I16	0.67	0.66	0.65	0.65	0.66	0.7	0.69
I17	0.54	0.55	0.61	0.51	0.53	0.57	0.55
I18	0.47	0.5	0.48	0.47	0.48	0.52	0.49

The data in Table 1 was obtained without rotation and scaling. The diagonal elements in Table 1 correspond to the maximum value of the correlation coefficient. Rotating and scaling reduce the correlation coefficient estimate to 0.95. Computer simulation made it possible to estimate the probability of correct detection of the handgun, which was 0.882 for false alarm probability equal to 0.01. The non-detected weapons (and correspondingly low correlation coefficient) in Table 2 are due to the absence of etalons in the filter bank for tested images 1–7. The data in Table 2 was obtained for random values of rotation and scaling of tested images.

5. Conclusions

The paper concentrates on the synthesis and analysis of methods for handgun recognition while X-ray security system operation. The proposed method is based on a special image processing technique using a comparison of verified images with etalon images. The modeling gives the possibility to determine the probabilities of correct detection and false alarm (0.882 and 0.01, respectively). The future scope is associated with increasing the efficiency of detection by introducing new etalons and combining the correlation approach with the spectral technique of detection.

6. References

- [1] I. Ostroumov, K. Marais, N. Kuzmenko, Aircraft Positioning Using Multiple Distance Measurements and Spline Prediction, *Aviation*, 26(1) (2022) 1–10. doi: 10.3846/aviation.2022.16589.
- [2] S. Cusick, A. Cortes, C. Rodrigues, *Commercial Aviation Safety*, 6th ed., McGraw Hill, New York (2017).
- [3] I. Ostroumov, N. Kuzmenko, Configuration Analysis of European Navigational Aids Network, *Integr. Commun. Navig. Surveill. Conf. (ICNS)*, Dulles, VA, USA, (2021) 1–9. doi: 10.1109/ICNS52807.2021.9441576.
- [4] G.F. Titterton, *Aircraft Materials & Processes*, 5th ed., Sterling Book House, Mumbai, India, (2007).
- [5] O. Solomentsev et al., Data Processing Through the Lifecycle of Aviation Radio Equipment, 17th Int. Conf. Comput. Scis. Inf. Technols. (CSIT), Lviv, Ukraine, (2022,) 146–151. doi: 10.1109/CSIT56902.2022.10000844.
- [6] M. Zaliskyi et al., Model Building for Diagnostic Variables During Aviation Equipment Maintenance, 17th Int. Conf. Comput. Scis. Inf. Technols. (CSIT), Lviv, Ukraine, (2022) 160–164. doi: 10.1109/CSIT56902.2022.10000556.
- [7] E. Salas, D. Maurino, *Human Factors in Aviation*, 2nd ed., Academic Press, Burlington, (2010).
- [8] Y. Averyanova et al., Turbulence Detection and Classification Algorithm Using Data from AWR, 2022 IEEE Ukrainian Microw. Week (UkrMW), Kyiv (2022) 1–5.
- [9] I. Ostroumov, N. Kuzmenko, Statistical Analysis and Flight Route Extraction from Automatic Dependent Surveillance-Broadcast Data, *Integr. Commun. Navig. Surveill. Conf. (ICNS)*, Dulles, VA, USA, (2022) 1–9. doi: 10.1109/ICNS54818.2022.9771515.
- [10] K. Sweet, *Aviation and Airport Security. Terrorism and Safety Concerns*, CRC Press, Taylor & Francis Group, Boca Raton, (2008).
- [11] S. Gnatyuk, Critical Aviation Information Systems Cybersecurity, *Meet. Secur. Challs. Thr. Data Anals. Decis. Support*, 47(3) (2016) 308–316. doi: 10.3233/978-1-61499-716-0-308.
- [12] K. Khorolska, et al., Application of a Convolutional Neural Network with a Module of Elementary Graphic Primitive Classifiers in the Problems of Recognition of Drawing Documentation and Transformation of 2D to 3D Models, *Journal of Theoretical and Applied Information Technology* 100(24) (2022) 7426–7437.
- [13] Z. B. Hu, et al., Authentication System by Human Brainwaves Using Machine Learning and Artificial Intelligence, in: *Advances in Computer Science for Engineering and Education IV* (2021) 374–388. doi: 10.1007/978-3-030-80472-5_31
- [14] D. Mery, D. Saavedra, M. Prasad, X-Ray Baggage Inspection With Computer Vision: A Survey, *IEEE Access*, 8 (2020) 145620–145633. doi: 10.1109/ACCESS.2020.3015014.
- [15] V. Rizzo, D. Mery, Automated Detection of Threat Objects Using Adapted Implicit Shape Model, *IEEE Trans. Syst. Man Cybern. Syst.* 46(4) (2016) 472–482. doi: 10.1109/TSMC.2015.2439233.
- [16] R. Voliansky, A. Pranolo, Parallel Mathematical Models of Dynamic Objects, *Int. J. Adv. Intell. Inform.* 4(2) (2018) 120–131. doi: 10.26555/ijain.v4i2.229.
- [17] O. Solomentsev, et. al., Data Processing Method for Deterioration Detection During Radio Equipment Operation, *Workshop Microw. Theory Techs. Wirel. Commun. (MTTW)*, Riga, Latvia, (2019) 1–4. doi: 10.1109/MTTW.2019.8897232.
- [18] I. Ostroumov et al., Relative Navigation for Vehicle Formation Movement, 3rd KhPI Week on Adv. Tech. Kharkiv, Ukraine, (2022) 1–4. doi: 10.1109/KhPIWeek57572.2022.9916414.
- [19] O. Solomentsev, et. al., Sequential Procedure of Change-point Analysis During Operational Data Processing, *Workshop Microw. Theory Techs. Wirel. Commun. (MTTW)*, Riga, Latvia, (2020) 168–171. doi: 10.1109/MTTW51045.2020.9245068.
- [20] I. Prokopenko, I. Omelchuk, M. Maloyed, Synthesis of Signal Detection Algorithms Under Conditions of Aprioristic Uncertainty, *Ukrainian Microw. Week*, Kharkiv, Ukraine, (2020) 418–423. doi: 10.1109/UkrMW49653.2020.9252687.
- [21] N. Kuzmenko et al., Airplane Flight Phase Identification Using Maximum Posterior Probability Method, *IEEE 3rd Int. Conf. Syst. Anal. Intell. Comput.*

- (SAIC), Kyiv, Ukraine, (2022) 1–5. doi: 10.1109/SAIC57818.2022.9922913.
- [22] R. Alberts, Modeling and Control of Image Processing for Interventional X-Ray, Technische Universiteit Eindhoven, Eindhoven, (2010).
- [23] R. Gonzalez, R. Woods, Digital Image Processing, 4th ed., Pearson, New York, (2017).
- [24] W. Burger, M.J. Burge, Principles of Digital Image Processing: Core Algorithms, Springer, London, (2010).
- [25] O. Semenov, Aviation Security Equipment, NAU, Kyiv, Ukraine, (2013).
- [26] S. Sarkar, et. al., Design of Weapon Detection System, 3rd Conf. Electrons Sustain. Comm. Syst., Coimbatore, India, (2022) 1016–1022. doi: 10.1109/ICESC54411.2022.9885601.
- [27] S. Thaiparnit, N. Chumuang, M. Ketcham, Weapon Detector System by using X-Ray Image Processing Technique, 18th Int. Symp. Commun. Inf. Technol. (ISCIT), Bangkok, Thailand, (2018) 214–219. doi: 10.1109/ISCIT.2018.8587853.
- [28] S. Akçay, et. al., Transfer Learning Using Convolutional Neural Networks for Object Classification Within X-Ray Baggage Security Imagery, Int. Conf. Image Process. (ICIP), Phoenix, USA, (2016) 1057–1061. doi: 10.1109/ICIP.2016.7532519.
- [29] B. Gu, et. al., Automatic and Robust Object Detection in X-Ray Baggage Inspection Using Deep Convolutional Neural Networks, IEEE Trans. Ind. Electron. 68(10) (2021) 10248–10257. doi: 10.1109/TIE.2020.3026285.
- [30] Y. Gaus, et. al., Evaluation of a Dual Convolutional Neural Network Architecture for Object-Wise Anomaly Detection in Cluttered X-Ray Security Imagery, Int. Jt. Conf. Neural Netws. (IJCNN), Budapest, Hungary, (2019) 1–8. doi: 10.1109/IJCNN.2019.8851829.
- [31] J. Zhang, et. al., X-Ray Image Recognition Based on Improved Mask R-CNN Algorithm, Math. Probls. Eng. (2021) 1–14. doi: 10.1155/2021/6544325.
- [32] V. Larin et al., Prediction of the Final Discharge of the UAV Battery Based on Fuzzy Logic Estimation of Information and Influencing Parameters, 3rd KhPI Week on Adv. Technol., Kharkiv, Ukraine, (2022) 1–6. doi: 10.1109/KhPIWeek57572.2022.9916490.
- [33] O. Sushchenko et al., Airborne Sensor for Measuring Components of Terrestrial Magnetic Field, 41st Int. Conf. Electron. Nanotechnol. (ELNANO), Kyiv, Ukraine, (2022) 687–691. doi: 10.1109/ELNANO54667.2022.9926760.
- [34] O. Sushchenko et al., Integration of MEMS Inertial and Magnetic Field Sensors for Tracking Power Lines, XVIII Int. Conf. Perspect. Technol. Methods MEMS Des. (MEMSTECH), Polyana (Zakarpattya), Ukraine, (2022) 33–36. doi: 10.1109/MEMSTECH55132.2022.10002907.
- [35] R. Volianskyi, et. al., Dual Channel Sliding Mode Control for Chua’s Circuit, Workshop Adv. Wirel. Opt. Commun. (RTUWO), Riga, (2018) 112–117. doi: 10.1109/RTUWO.2018.8587912.
- [36] F. Yanovsky, I. Braun, Models of Scattering on Hailstones in X-band, First European Radar Conf., Amsterdam, Netherlands (2004) 229–232.
- [37] J. Al-Azzeh, et. al., A Method of Accuracy Increment Using Segmented Regression, Algorithms, 15(10) 378 (2022) 1–24. doi: 10.3390/a15100378.
- [38] D. Hearn, M. Baker, W. Carithers, Computer Graphics with OpenGL, 4th ed., Pearson, New York (2014).